A proxy index of ENSO teleconnections from the central equatorial Pacific

Variations in central and eastern equatorial sea surface temperatures are linked to extratropical climate anomalies via atmospheric water vapor and heat fluxes[1,2]. Here we reconstruct a measure of central equatorial Pacific SST anomaly for 1938-1993 from stable isotopic ($\delta^{18}O$) results from a coral collected at Kiritimati (Christmas) Island, Republic of Kiribati (157.3ºW, 2ºN), in one of the most data-poor regions of the tropical oceans. We recover not only regional SST anomaly, but also extratropical climate information in teleconnected regions.

Sea surface temperature estimates may be derived from the isotopic composition and minor-element chemistry of aragonite formed by annually-banded reef corals. Interannual variability in the oxygen isotopic composition ($\delta^{18}O$) is a function of the SST in which the coral secreted its skeleton[3], but depending on the oceanographic setting, may also record changes in the $\delta^{18}O$ of sea water[4]. The Strontium:Calcium (Sr/Ca) ratio in corals has been shown to be a function of SST, with minimal sea water Sr/Ca influence[5,6]. Application of these two tracers in tandem has been used to distinguish sea water $\delta^{18}O$ and sea surface temperature anomalies recorded on the Great Barrier Reef during the 1982-3 El Niño-Southern Oscillation (ENSO) event[7]. In principle, paired Sr/Ca and $\delta^{18}O$ data from a series of temporally-overlapping coral cores may be used to construct proxy records of SST and sea surface salinity variability well into the pre-instrumental period.

At Kiritimati, the seasonal SST cycle is modest (≤1.2ºC), while ENSO warm and cold phase SST anomalies of ±3ºC are prominent and reflect changes in wind stress and associated equatorial upwelling[8]. Thus, Kiritimati is an ideal location at which to monitor the thermal oceanographic signal associated with the full ENSO cycle. We measured $\delta^{18}O$ and $\delta^{13}C$ on a core from a living coral collected in March 1994, at 0.5mm intervals along the maximal growth axis of the coral. The $\delta^{13}C$ record was used to construct an age model for time series analysis of the $\delta^{18}O$ record, based on observations of the dependence of $\delta^{13}C$ of coralline aragonite on coralline reproductive activity[9]. This sampling resolution enabled us to obtain 25-35 samples per annual band and achieve a chronology with better than monthly resolution and low age model error estimates[10] (Fig. 1A). Paired $\delta^{18}O$ and Sr/Ca results and SST data for the 1981-86 period confirm that both geochemical thermometers have captured the interannual SST variability over this 6 year period, which includes the strong ENSO warm event of 1982-3, normal/cold conditions through mid-1986, and the initiation of the 1986-7 warm phase event (Fig. 1B). As our interest here is in the interannual variability, we analyze further only April-March annual averages of the oxygen isotopic record, which we term “NINO-C” and interpret as primarily driven by SST anomaly (Fig. 1C). NINO-C shares over 60% variance with the commonly used NINO3 area index (150^{o}W-90^{o}W, 5^{o}N-5^{o}S) of eastern equatorial Pacific SST[10].

NINO-C should also provide a good index of teleconnections associated with ENSO, since SST extrema in the central equatorial Pacific directly influence the atmospheric circulation[1,2]. Analysis of surface meteorological station - NINO-C correlation patterns indicates that global, interannual patterns of surface air temperature and precipitation anomaly are recoverable from NINO-C (Fig. 2) in the Americas, Africa, Australia, India, and Southeast Asia. These patterns generally agree, in both spatial distribution and correlation amplitude, with those recovered by correlation of station data with like averages of NINO3 and with the literature on tropical-extratropical climate teleconnections[1,2,11-13]. However, correlations with NINO3 are stronger than correlations with NINO-C in the southeast U.S. for both temperature and precipitation, suggesting this region is more sensitive to SST variability in the eastern than the central equatorial Pacific, while surface temperatures in central and northeastern Asia at about 45^{o}N appear responsive to NINO-C, but not to NINO3. These results suggest overall similarity but also subtle differences between teleconnections associated with the central and eastern equatorial Pacific regions, which may be resolved by indices from the central equatorial Pacific and other data-poor regions of the tropical oceans.

We have shown that NINO-C is capable of providing a record of both tropical and extratropical climate variability on interannual time scales; hence, comparison of modern and paleoclimatic NINO-C results will permit analysis of climate change relative to the present, in both the central equatorial Pacific and in teleconnected regions. Seasonally-variant carbon isotopic composition or density banding provides a relative chronology for a coral colony's lifetime, while absolute dating of fossil coral samples can be achieved via the radiocarbon or U-series techniques. By these means, multi-proxy extension of NINO-C into the pre-instrumental period will permit exploration of links to documented extratropical paleoclimate anomalies on interdecadal time scales.

M.N. Evans*, R.G. Fairbanks*, J.L. Rubenstone

Lamont-Doherty Earth Observatory of Columbia University, Palisades, NY 10964-8000

**Also at: Dept. of Earth and Environmental Sciences, Columbia University, NY, NY 10027*

Data presented in this paper is available from the authors (email: mevans@ldeo.columbia.edu), Nature, or the World Data Center A - for Paleoclimatology (www.ngdc.noaa.gov/paleo). LDEO contribution #5812.

References

1. Pan, Y. & Oort, A. *Mon. Weath. Rev.* **111**, 1244-1258 (1983).

2. Graham, N. & Barnett, T. *Science* **238**, 657-659 (1987).

3. Weber, J. & Woodhead, P. *J. Geophys. Res.* **77**, 463-473 (1972).

4. Cole, J., Fairbanks, R.G. & Shen, G.T. *Science* **260**, 1790-1793 (1993).

5. Weber, J. *Geochim. et Cosmochim. Acta* **37**, 2173-2190 (1973).

6. DeVilliers, S., Shen, G.T. & Nelson, B.K. *Geochim. et Cosmochim. Acta* **58**, 197-208 (1994).

7. McCulloch, M., Gagan, M., Mortimer, G., Chivas, A. & Isdale, P. *Geochim. et Cosmochim. Acta* **58**, 2747-2754 (1994).

8. Philander, S. G.H. *El Niño, La Niña, and the Southern Oscillation* (Academic Press, San Diego, 1990).

9. Gagan, M., Chivas, A. & Isdale, P. *Geology* **24**, 1009-1012 (1996).

10. Evans, M., Fairbanks, R.G. & Rubenstone, J.L. *J. Geophys. Res.* (1998), submitted; preprint available at http://rainbow.ldeo.columbia.edu/~mevans/preprints/.

11. Ropelewski, C.F. & Halpert, M.S. *Mon.Wea. Rev.* **114**, 2352-2362 (1987).

12. Ropelewski, C.F. & Halpert, M.S. *J. Climate* **2**, 268-284 (1989).

13. Halpert, M. & Ropelewski, C. *J. Climate* **5**, 577--593 (1992).

14. Reynolds, R.W. & Smith, T.M. *J. Climate* **7**, 929--948 (1994).

15. Baker, C., Eischeid, J., Karl, T. & Diaz, H. in *Preprints of AMS Ninth Conference on Applied Climatology, Dallas, TX., January 15-20 , 1995* . Data accessed via the LDEO climate server (http://ingrid.ldgo.columbia.edu/SOURCES/.NOAA/.NCDC/.GCPS/).

Figure Captions

Figure 1A Kiritimati coral $\delta^{18}O$ time series normalized to the 1951-80 mean and standard deviation of the data. $\delta^{18}O$ scale has been reversed. Error bars give uncertainty in $\delta^{18}O$ and decadal averages of age model uncertainty estimates[10].

Figure 1B Kiritimati coral $\delta^{18}O$ (‰, PDB scale; blue circles) and Sr/Ca anomalies (mmol/mol; red circles) relative to the mean for the 1981-1987 period. Reproducibility confidence intervals (estimated 2σ) for each tracer are as indicated. Also plotted (black line) are sea surface temperature anomaly estimates from the analysis by Reynolds and Smith[14] for the 2^{o} x 2^{o} grid box encompassing Kiritimati. The data have been plotted on a common range so that direct comparisons of the different measurements may be made: 8^{o} C ≈1.6‰ in $\delta^{18}O$ ≈ 0.6 mmol/mol in Sr/Ca[3,6].

Figure 1C Plot of NINO-C (red line) and NINO3 index (SST anomaly averaged over 150^{o}W-90^{o}W, 5^{o}N-5^{o}S; black line) vs. time. Also shown are the number of samples analyzed per year and SST observations, respectively. Correlation between NINO-C and NINO3 is -0.79.

Figure 2 Linear correlations (r) between -1*NINO-C and (**A**) surface air temperature and (**B**) precipitation data from a global network of stations[15]. The locations of all stations with ≤ 42 years of data are plotted in grey; stations correlated at or above the 90% confidence level ($|r| \geq 0.3$; ≈ 36 degrees of freedom) are plotted in color. In general the recovered patterns agree with those recovered by correlation with like averages of NINO3, although there are subtle differences (see text).

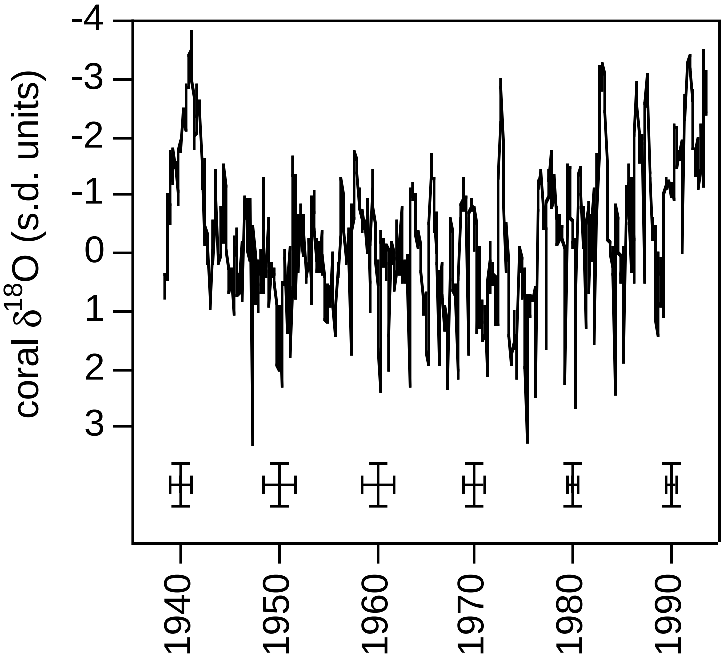

Figure 1A

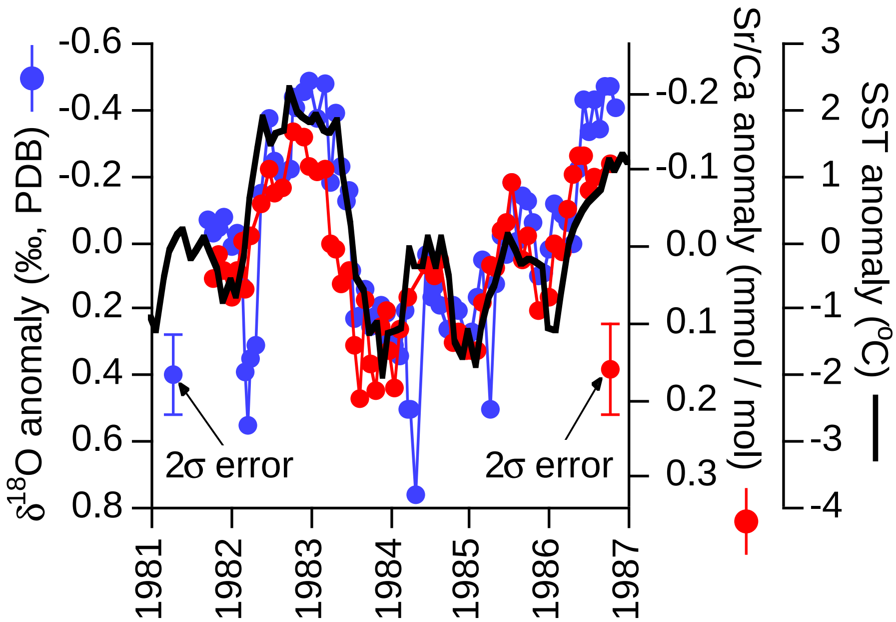

Figure 1B

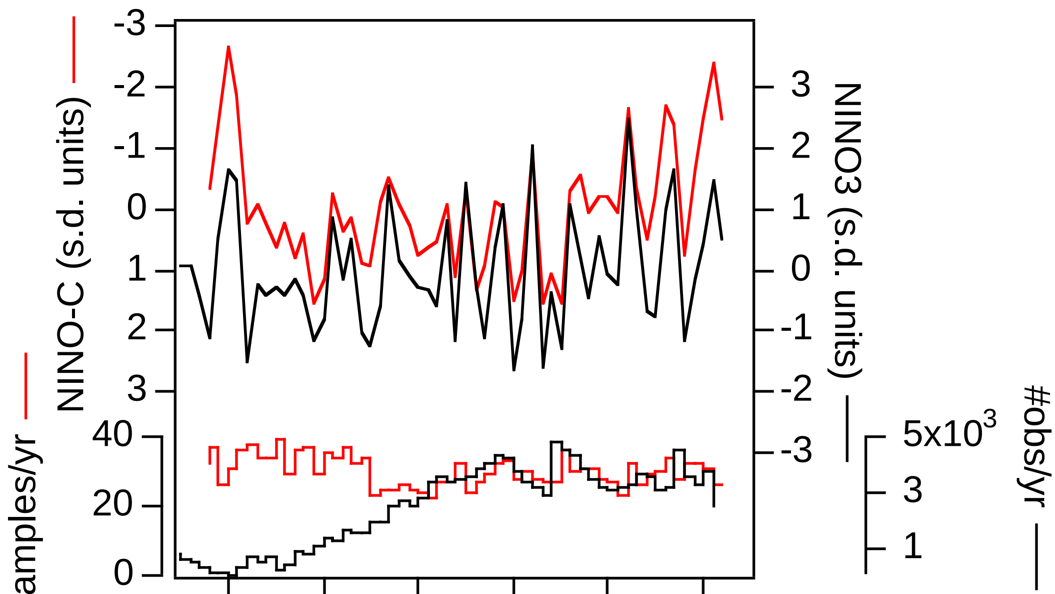

Figure 1C

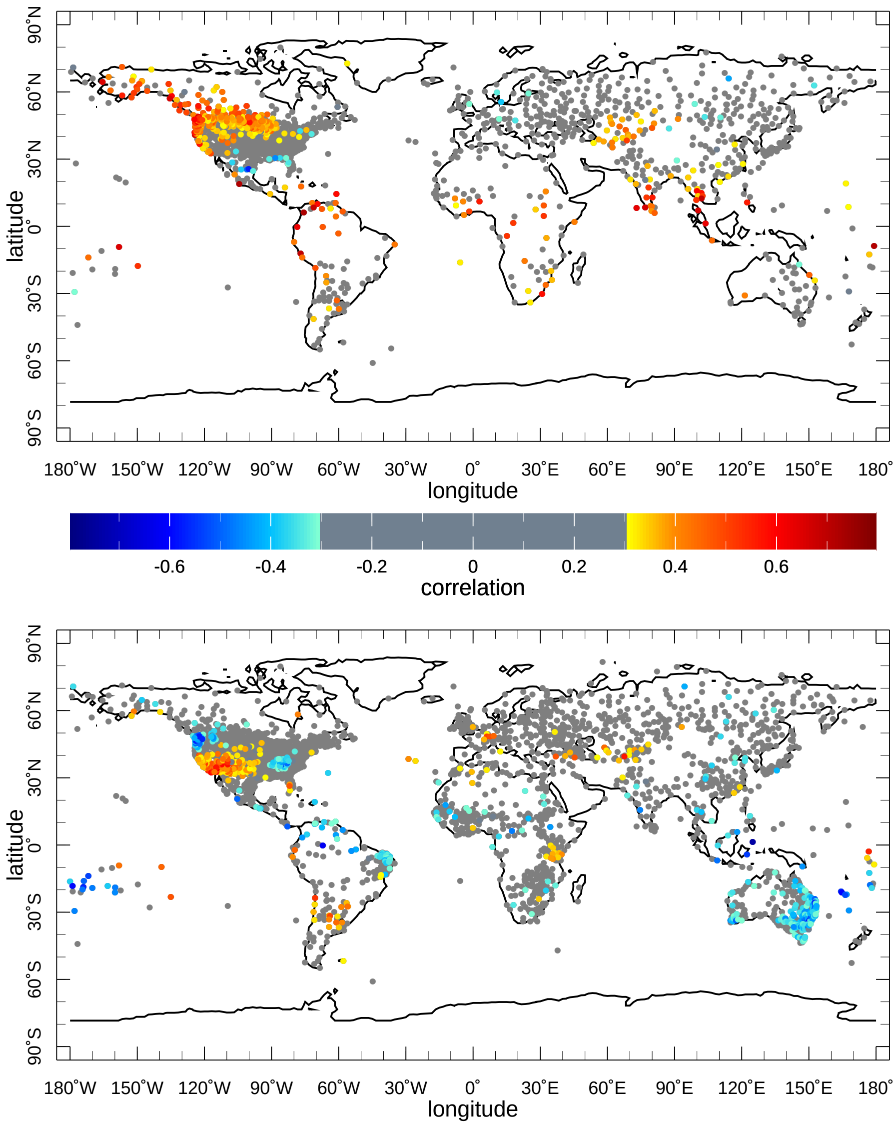

90°N
60°N
30°N
0°
30°S
60°S
90°S
latitude
180°W 150°W 120°W 90°W 60°W 30°W 0° 30°E 60°E 90°E 120°E 150°E 180°
longitude
-0.6 -0.4 -0.2 0 0.2 0.4 0.6
correlation
90°N
60°N
30°N
0°
30°S
60°S
90°S
latitude
180°W 150°W 120°W 90°W 60°W 30°W 0° 30°E 60°E 90°E 120°E 150°E 180°
longitude

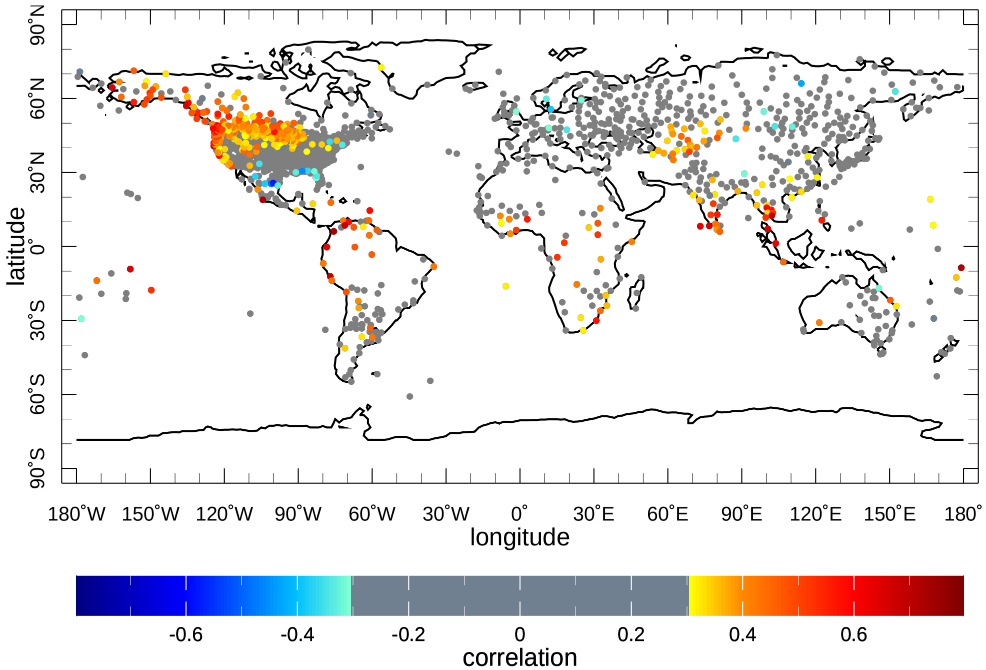

Figure 3B. correlation of NINO3 SST and surface air temperature

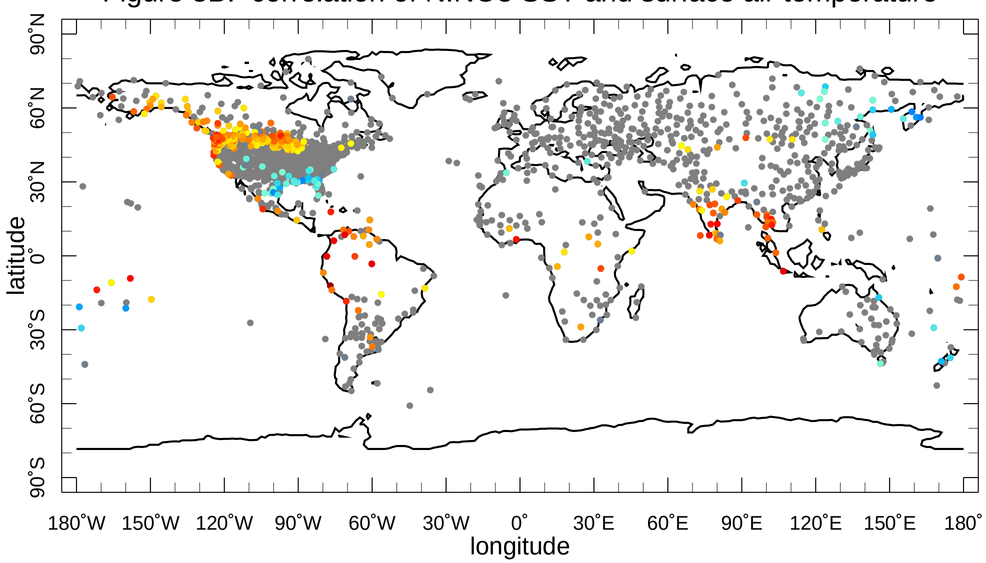

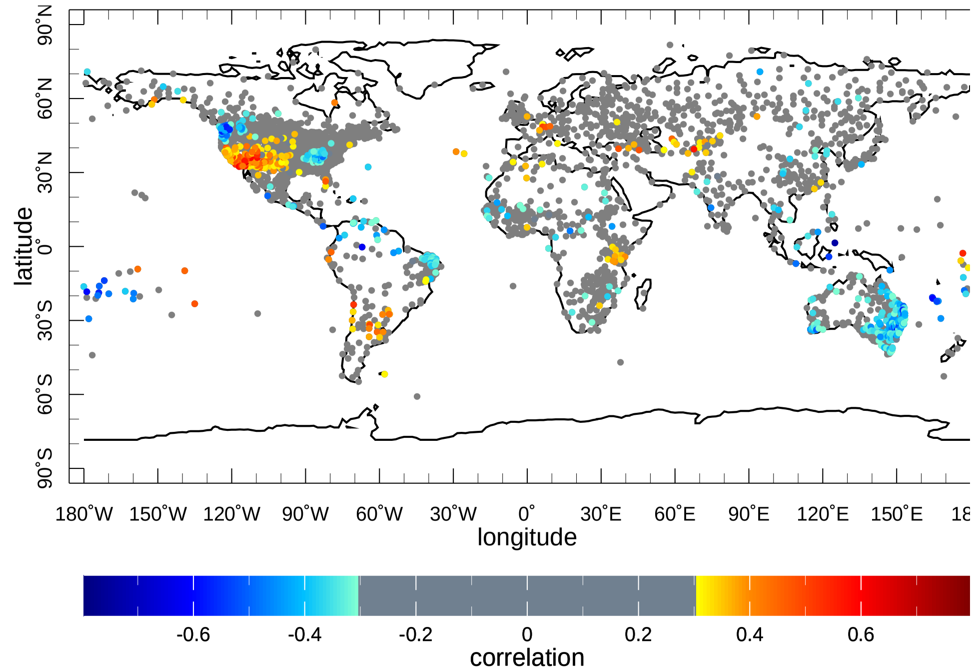

Figure 3D. correlation of NINO3 SST and precipitation